PNAS RESEARCH ARTICLE | IMMUNOLOGY AND INFLAMMATION

Hypoxia inducible factor 2α promotes tolerogenic macrophage development during cardiac transplantation through transcriptional regulation of colony stimulating factor 1 receptor

Matthew DeBerge[a,b,1,2], Samantha Schroth[a,1], Fanfan Du[c], Xin Yi Yeap[a], Jiao-Jing Wang[d], Zheng Jenny Zhang[d], Mohammed Javeed Ansari[e], Evan A. Scott[c], and Edward B. Thorp[a,2]

Affiliations are included on p. 11.

Edited by Megan Sykes, Columbia University, New York, NY; received November 17, 2023; accepted May 20, 2024 by Editorial Board Member Carl F. Nathan

Solid organ transplantation mobilizes myeloid cells, including monocytes and macrophages, which are central protagonists of allograft rejection. However, myeloid cells can also be functionally reprogrammed by perioperative costimulatory blockade to promote a state of transplantation tolerance. Transplantation tolerance holds promise to reduce complications from chronic immunosuppression and promote long-term survival in transplant recipients. We sought to identify different mediators of transplantation tolerance by performing single-cell RNA sequencing of acute rejecting or tolerized cardiac allografts. This led to the unbiased identification of the transcription factor, hypoxia inducible factor (HIF)-2α, in a subset of tolerogenic monocytes. Using flow cytometric analyses and mice with conditional loss or gain of function, we uncovered that myeloid cell expression of HIF-2α was required for costimulatory blockade–induced transplantation tolerance. While HIF-2α was dispensable for mobilization of tolerogenic monocytes, which were sourced in part from the spleen, it promoted the expression of colony stimulating factor 1 receptor (CSF1R). CSF1R mediates monocyte differentiation into tolerogenic macrophages and was found to be a direct transcriptional target of HIF-2α in splenic monocytes. Administration of the HIF stabilizer, roxadustat, within micelles to target myeloid cells, increased HIF-2α in splenic monocytes, which was associated with increased CSF1R expression and enhanced cardiac allograft survival. These data support further exploration of HIF-2α activation in myeloid cells as a therapeutic strategy for transplantation tolerance.

macrophage | transplant | tolerance

Significance

Transplantation tolerance holds promise to reduce complications from chronic immunosuppression and promote long-term survival in transplant recipients. Our findings reveal that transplantation tolerance requires unique signaling in monocytes to promote their differentiation into tolerogenic macrophages. This mechanism in transplantation tolerance has implications in other settings of immune tolerance, including pregnancy and cancer, and supports its therapeutic activation in the setting of heart transplantation to promote long-term survival in humans.

Heart transplantation has emerged as a routine, therapeutic option for end-stage heart failure patients unresponsive to other forms of treatment (1). Clinical progress has reduced acute rejection, yet long-term survival remains poor because complications of chronic immune suppression often lead to significant comorbidities, including posttransplant vasculopathy (2). Furthermore, chronic immune suppression during transplant raises risks for opportunistic infections (3) and adverse hematologic, metabolic, or nephrotoxic events (4). An alternative to chronic immunosuppressive therapy is transplantation tolerance, which is characterized by donor-specific immunological unresponsiveness in the absence of immunosuppressive medications (5). Transplantation tolerance holds promise in promoting long-term survival by eliminating the need for chronic immunosuppression and its associated complications.

Studies have shown that myeloid cells, including monocytes and macrophages, are required for immunological tolerance induced by costimulatory blockade in cardiac allografts (6). For example, treatment of mice with antibodies blocking lymphocyte expression of the costimulatory molecule, CD40 ligand (CD40L), results in long-term cardiac allograft survival (7), which was abrogated upon antibody or pharmacologic depletion of myeloid cells (8). Similar requirements for myeloid cells in costimulatory blockade–induced transplantation tolerance were also observed in kidney (9) or skin allografts (10). Within cardiac allografts, accumulation of tolerogenic macrophages was found to be dependent on recruitment of monocytes from peripheral reservoirs such as the bone marrow (11). Monocyte differentiation into tolerogenic macrophages required colony stimulating factor 1 (CSF1) signaling through its cognate receptor, CSF1R (11). In contrast, mammalian target of rapamycin (mTOR) and TNF receptor associated factor 6 (TRAF6) signaling have been implicated in differentiation of monocytes into graft rejecting, immunogenic macrophages (12).

Author contributions: M.D., S.S., M.J.A., and E.B.T. designed research; M.D., S.S., X.Y.Y., J.-J.W., Z.J.Z., and M.J.A. performed research; F.D., Z.J.Z., and E.A.S. contributed new reagents/analytic tools; M.D., S.S., and E.B.T. analyzed data; and M.D., S.S., F.D., E.A.S., and E.B.T. wrote the paper.

The authors declare no competing interest.

This article is a PNAS Direct Submission. M.S. is a guest editor invited by the Editorial Board.

[1]M.D. and S.S. contributed equally to this work.

[2]To whom correspondence may be addressed. Email: Matthew.P.DeBerge@uth.tmc.edu or ebthorp@northwestern.edu.

This article contains supporting information online at https://www.pnas.org/lookup/suppl/doi:10.1073/pnas.2319623121/-/DCSupplemental.

Published June 18, 2024.

To assess mechanisms governing the generation of tolerogenic macrophages, we performed single-cell RNA sequencing on cardiac allografts during acute rejection or transplantation tolerance. This led to the unbiased identification of *Endothelial PAS domain-containing protein 1* (*Epas1*), in a subset of cardiac monocytes present only during transplantation tolerance. *Epas1* encodes the transcription factor, hypoxia inducible factor 2α (HIF-2α), which had been shown to promote tumorigenesis in part through macrophage expression of CSF1R (13). Genetic deletion of *Epas1* in myeloid cells abrogated cardiac transplantation tolerance induced by costimulatory blockade and this was associated with reduced expression of CSF1R on tolerogenic monocytes and macrophages. HIF-2α was found to directly bind to the *Csf1r* promotor in tolerogenic monocytes and therapeutic activation of HIF-2α enhanced monocytic CSF1R expression and cardiac allograft survival. As discussed in further detail below, our findings reveal that HIF-2α is required for the development of tolerogenic macrophages and its therapeutic activation holds promise in cardiac transplantation tolerance.

Results

To identify myeloid-specific factors that are required for cardiac transplantation tolerance, we performed single-cell RNA sequencing on magnetically enriched CD45$^+$ hematopoietic cells from acute rejecting or tolerized cardiac allografts (Fig. 1*A*). Unbiased clustering of cells combined from both groups revealed a diverse array of cell populations, including innate and adaptive immune cells, as well as stromal and endothelial cells (Fig. 1*B*). We next rescaled and reclustered all monocyte and macrophage subsets from both groups, which led to the identification of six transcriptionally distinct clusters (Fig. 1 *C* and *D*). Macrophages were identified using canonical markers such as *Adgre1* and *Mertk*, while monocytes were identified by expression of *Ly6c1* and *Ccr2* (Fig. 1*E*). When we examined the proportion of monocyte and macrophage clusters between acute rejection and tolerized cardiac allografts, we found that *Pkm* macrophages comprised the majority of cells within acute rejecting allografts, whereas tolerized allografts were characterized by increased abundance of *Mrc1* macrophages and *Ly6c1* monocytes (Fig. 1 *F* and *G*). Pathway analyses revealed that *Pkm* macrophages were enriched in immunogenic processes, such as response to interferon (IFN)-γ and inflammatory response (Fig. 1*H*). In contrast, tolerogenic *Mrc1* macrophages and *Ly6c1* monocytes were enriched for homeostatic, developmental, and biosynthetic processes (Fig. 1*H*). Interestingly, examination of canonical "M1" or "M2" marker gene expression between *Pkm* and *Mrc1* macrophage clusters revealed heterogeneity beyond the classical M1/M2 paradigm (*SI Appendix*, Fig. S1 *A and B*), supporting distinct transcriptional reprogramming during transplantation tolerance compared to acute rejection.

Since Ly6C^{hi} monocytes have been found to differentiate into tolerogenic macrophages within cardiac allografts (11), we continued to explore the relationship between tolerogenic *Ly6c1* monocytes and *Mrc1* macrophages. Tolerogenic *Ly6c1* monocytes were enriched in genes involved in cell differentiation (Fig. 1*H*) and expressed high levels of *Fabp4* and *Cd36* (Fig. 1*I*), which are up-regulated in monocytes differentiating into macrophages (14). Furthermore, tolerogenic *Mrc1* macrophages displayed high levels of *Ccr2* and *Cx3cr1* (Fig. 1*I*), indicative of a monocytic origin. Tolerogenic *Mrc1* macrophages also expressed *Nr4a1*, which is required for Ly6C^{hi} monocyte differentiation into Ly6C^{lo} macrophages in the heart (15). To determine whether tolerogenic *Ly6c1* monocytes developed into *Mrc1* macrophages, we used the Monocle algorithm to map pseudotime (16), or the progression of gene expression changes that a cell undergoes to transition from one functional state to another. This revealed that tolerogenic *Ly6c1* monocytes followed a developmental trajectory that gave rise to *Mrc1* macrophages (Fig. 2*A*). Tracking of gene expression changes over pseudotime also revealed that tolerogenic *Ly6c1* monocytes increased expression of macrophage marker genes, *Adgre1, Cd68, Mertk*, as well as *Csf1r* and *Ccr2* on their developmental path to *Mrc1* macrophages (Fig. 2*B*).

After establishing a hypothetical relationship between tolerogenic *Ly6c1* monocytes and *Mrc1* macrophages, we next asked whether there was a definitive relationship between these two populations. Since *Ly6c1* monocytes expressed *Ccr2* during macrophage differentiation and CCR2 is required for Ly6C^{hi} monocyte recruitment during cardiac inflammation (17, 18), we treated congenic recipient mice with a CCR2-specific inhibitor during transplantation tolerance to determine the contribution of peripheral monocytes to tolerogenic macrophages within the allograft (Fig. 2*C*). After transplanting cardiac allografts from CD45.2 donors into CD45.1 recipients, we found that nearly all the CD11b$^+$ myeloid cells within the tolerized allograft were recipient-derived a week after transplantation (Fig. 2*D*). Treatment of tolerized donors with a CCR2 inhibitor reduced total abundance of recipient-derived CD11b$^+$ myeloid cells and Ly6C^{hi} monocytes within the allograft (Fig. 2 *E* and *F*). *Mrc1* encodes the mannose receptor, also known as CD206, and recipient-derived CD206$^+$ macrophages were also reduced in tolerized allografts after CCR2 inhibition (Fig. 2*G*), suggesting that Ly6C^{hi} monocytes differentiated into CD206$^+$ macrophages within the allograft during transplantation tolerance.

To identify the source of these tolerogenic monocytes, we examined changes in monocyte numbers within the spleen, as this organ serves as a reservoir for Ly6C^{hi} monocytes during cardiac inflammation (19). Ly6C^{hi} monocyte abundance increased in the spleen during transplantation tolerance, which was further enhanced during CCR2 inhibition (Fig. 2*H*), identifying the spleen as a reservoir of tolerogenic monocytes. To test the requirements of CCR2-dependent monocyte recruitment for costimulatory blockade–induced transplantation tolerance, we transplanted hearts into *Ccr2*-deficient recipients or controls (Fig. 2*I*). While costimulatory blockade–induced transplantation tolerance provided durable survival in wild-type controls, loss of *Ccr2* abrogated transplantation tolerance induction (Fig. 2*J*), which was associated with increased vasculopathy (Fig. 2*K*). Prior to rejection, the abundance of total viable cells was reduced in allografts of tolerized *Ccr2*−/− recipients with an increased percentage of dead cells compared to controls (*SI Appendix*, Fig. S2 *A* and *B*). Despite the reduction in cellularity, allografts from tolerized *Ccr2*−/− recipients exhibited increased neutrophil infiltration with similar changes also occurring during CCR2 inhibition (*SI Appendix*, Fig. S2 *C* and *D*). As expected, Ly6C^{hi} monocyte abundance was reduced in allografts from tolerized *Ccr2*−/− recipients (*SI Appendix*, Fig. S2*E*), which was associated with reduced accumulation of tolerogenic CD206$^+$ macrophages (*SI Appendix*, Fig. S2*F*) and increased expression of inflammatory markers on macrophages (*SI Appendix*, Fig. S2*G*). Together, this establishes Ly6C^{hi} monocytes as central mediators of transplantation tolerance.

Since Ly6C^{hi} monocytes were required for costimulatory blockade–induced cardiac transplantation tolerance, we next examined the top differentially expressed genes within the tolerogenic monocyte cluster to identify specific factors that were required for their tolerogenic function. Among the top 20 differentially expressed genes, *Epas1* was identified as the only gene to encode a transcription factor (Fig. 3*A*), so we continued to explore its role in tolerogenic monocytes. *Epas1* encodes the transcription factor, HIF-2α, which is best characterized for its role in regulating the physiological response to reduced oxygen concentration (20). Compared to the other myeloid cell clusters, the highest expression of *Epas1*

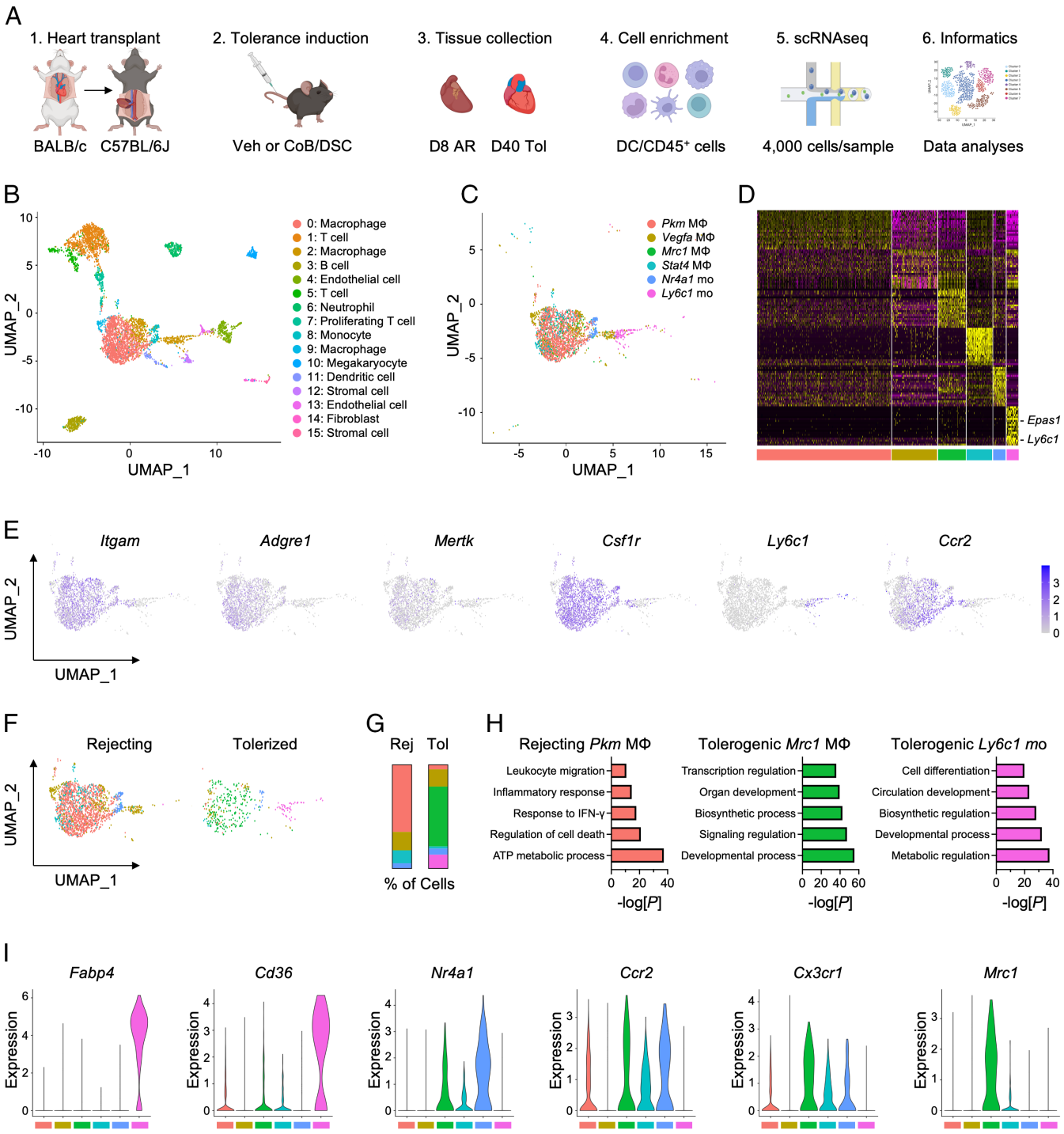

Fig. 1. Single-cell RNA sequencing (scRNAseq) of cardiac allografts during acute rejection or tolerance reveals unique populations of tolerogenic macrophages and monocytes. (*A*) Experimental design for scRNAseq of cardiac allografts. Allografts were collected either 8 d after transplant in vehicle-treated mice for acute rejection or 40 d after transplant in mice treated with costimulatory blockade (CoB) and donor-specific cells (DSC) for tolerance. (*B*) Identification of 16 unique clusters by uniform manifold approximation and projection (UMAP) in combined conditions. (*C*) Identification of six unique clusters of macrophages and monocytes in combined conditions. (*D*) Heatmap of the 20 most differentially expressed genes within macrophage and monocyte clusters. (*E*) Feature plots representing single-cell expression of macrophage and monocyte marker genes. (*F*) Macrophage and monocyte clusters present during acute rejection or tolerance. (*G*) Proportion of macrophage and monocyte clusters during acute rejection or tolerance. (*H*) Pathway enrichment of differentially expressed genes in macrophage and monocyte clusters. Enrichment is expressed as the −log(P) and is adjusted for multiple comparisons. (*I*) Violin plots of genes expressed in macrophage and monocyte clusters.

was observed in tolerogenic monocytes (Fig. 3*B*). In contrast, gene expression of *Hif1a*, which encodes the other major isoform of hypoxia inducible transcription factors, was reduced in tolerogenic monocytes compared to the other myeloid clusters (Fig. 3*C*). To determine the role of HIF-2α in tolerogenic monocytes during transplantation tolerance, we selectively deleted *Epas1* in myeloid cells (*mHIF2*−/−) by crossing transgenic mice with a floxed *Epas1* gene with mice expressing Cre recombinase under the control of the *Lyz2* promotor (Fig. 3*D*). While costimulatory blockade–induced transplantation tolerance provided durable survival in Cre negative, floxed controls, long-term allograft survival was impaired in *mHIF2*−/− recipients (Fig. 3*E*). Prior to rejection, cardiac allografts from tolerized *mHIF2*−/− recipients exhibited increased vasculopathy (Fig. 3*F*), revealing the requirement of

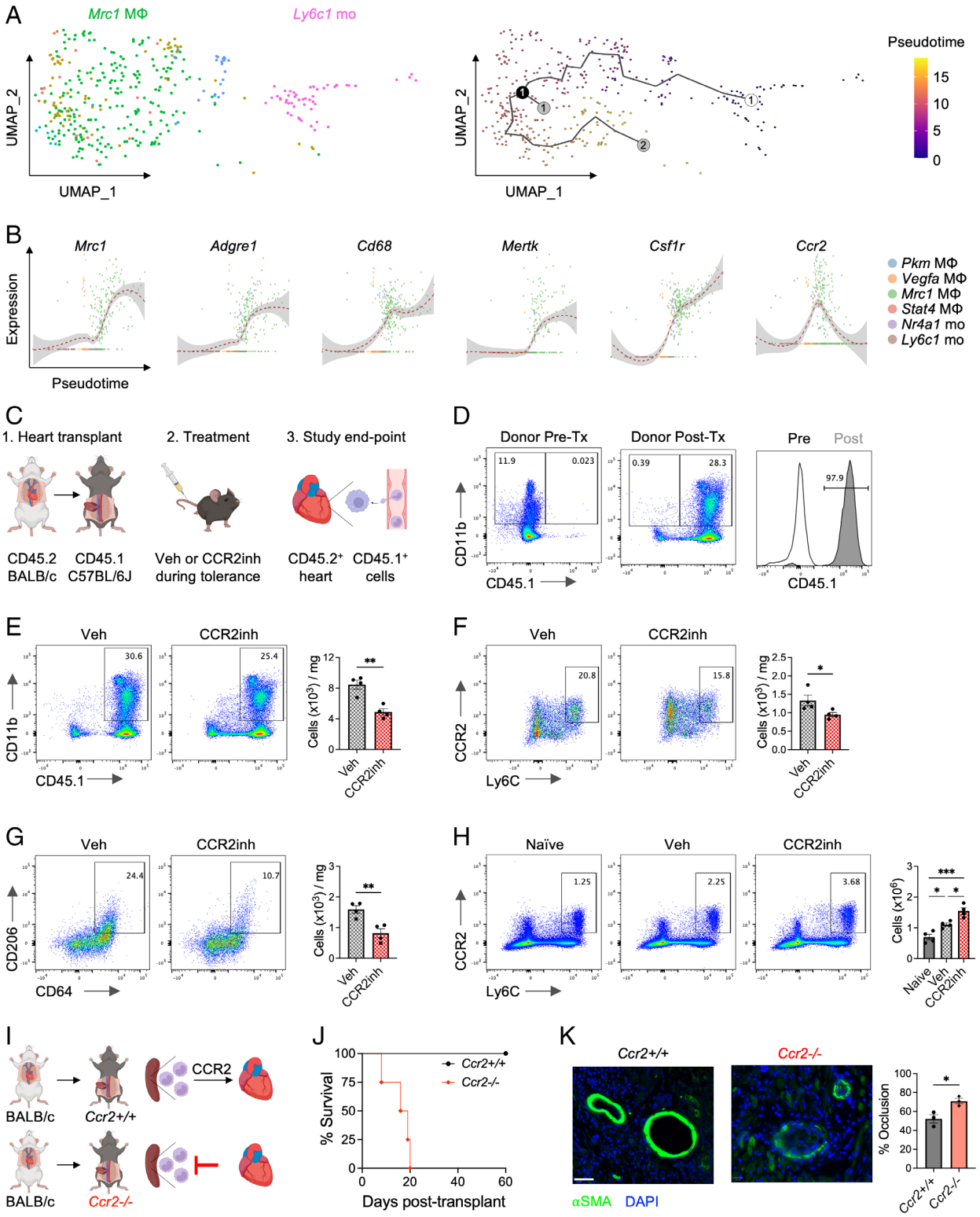

Fig. 2. CCR2-dependent monocyte recruitment to cardiac allografts is required for transplantation tolerance. (*A*) Pseudotime trajectory analysis of monocyte to macrophage differentiation during transplantation tolerance. The open circle is the start of the trajectory with the black line representing the different paths. The black circle represents a branch point, while the gray circles represent different cell fates. (*B*) Monocyte and macrophage gene expression plotted as a function of Pseudotime. (*C*) Experimental design for tracking recipient-derived CD45.1$^+$ monocytes and macrophages in CD45.2$^+$ cardiac allografts during transplantation tolerance. (*D*) Ratio of CD45.2$^+$ donor vs. CD45.1$^+$ recipient-derived myeloid cells in cardiac allografts 1 wk after transplantation. Total abundance of CD45.1$^+$ recipient-derived (*E*) CD11b$^+$ myeloid cells, (*F*) Ly6C^{hi} monocytes, and (*G*) CD206$^+$ macrophages in CD45.2$^+$ cardiac allografts 1 wk after transplantation in tolerized recipients treated with vehicle or CCR2 inhibitor. For (*E–G*), $n = 4$ mice/group pooled from two independent experiments. *$P < 0.05$ and **$P < 0.01$ by the two-tailed, unpaired *t* test (*H*) Ly6C^{hi} monocyte abundance in the spleen 1 wk after transplantation in tolerized recipients treated with vehicle or CCR2 inhibitor. $n = 4$ mice/group pooled from two independent experiments. *$P < 0.05$, ***$P < 0.001$ by one-way ANOVA followed by Tukey's test. (*I*) Experimental design for heart transplantation in tolerized *Ccr2*+/+ or *Ccr2*−/− recipients. (*J*) Cardiac allograft survival in tolerized *Ccr2*+/+ or *Ccr2*−/− recipients. $n = 4$ mice/group pooled from two independent experiments. **$P < 0.01$ by the log-rank (Mantel–Cox) test. (*K*) Expression of α-Smooth Muscle Actin (SMA) in cardiac allografts from tolerized *Ccr2*+/+ or *Ccr2*−/− recipients 60 d after transplantation with quantification of percent vessel occlusion. $n = 3$ mice/group pooled from two independent experiments. *$P < 0.05$ by the two-tailed, unpaired *t* test. (Scale bar, 40 μm.) All data represent mean ± SEM.

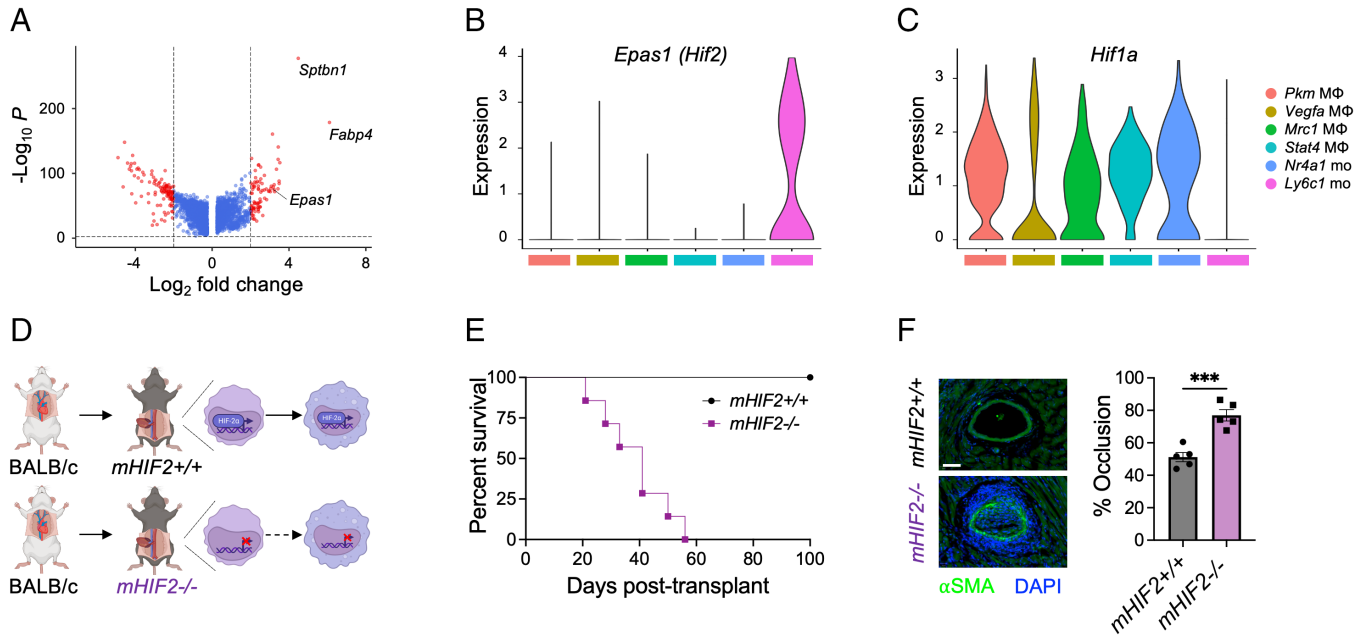

Fig. 3. Myeloid cell expression of HIF-2α is required for cardiac allograft transplantation tolerance. (*A*) Volcano plot of the top differentially expressed genes in tolerogenic *Ly6c1* monocytes. Violin plots of (*B*) *Epas1* (*Hif2*) and (*C*) *Hif1a* expression among myeloid cells in combined conditions. (*D*) Experimental design for heart transplantation in tolerized *LysMCre*$^{-}$*Hif2*^{flox} mice (*mHIF2+/+*) or *LysMCre*$^{+}$*Hif2*^{flox} (*mHIF2−/−*) recipients. (*E*) Cardiac allograft survival in tolerized *mHIF2+/+ or mHIF2−/−* recipients. *n* = 7 to 8 mice/group pooled from three independent experiments. ***$P < 0.001$ by the log-rank (Mantel–Cox) test. (*F*) Expression of α-Smooth Muscle Actin (SMA) in cardiac allografts from tolerized *mHIF2+/+* or *mHIF2−/−* recipients 30 d after transplantation with quantification of percent vessel occlusion. *n* = 5 mice/group pooled from two independent experiments. ***$P < 0.001$ by the two-tailed, unpaired *t* test. (Scale bar, 20 μm.)

myeloid HIF-2α in costimulatory blockade–induced cardiac transplantation tolerance.

Next, we sought to uncover how myeloid HIF-2α regulated the induction of transplantation tolerance. HIF-2α directly regulates the expression of *Cd36* (21), which was also increased in tolerogenic monocytes (Fig. 1*I*), and is required for monocyte to macrophage differentiation during cardiac inflammation (22). So, we next tested whether monocytic CD36 was required for transplantation tolerance. *Cd36* was selectively deleted in myeloid cells (*mCD36−/−*) by crossing transgenic mice with a floxed *Cd36* gene with mice expressing Cre recombinase under the control of the *Lyz2* promotor. However, no difference in allograft survival was observed between *mCD36−/−* recipients and controls (*SI Appendix*, Fig. S3), demonstrating that CD36 was not required for transplantation tolerance under these conditions.

Since myeloid CD36 was dispensable for transplantation tolerance, we next investigated how HIF-2α affected the extent and quality of myeloid cell infiltrate in the allograft after transplantation. Differentiation of monocytes into tolerogenic macrophages requires CSF1-CSF1R signaling (11), so we examined accumulation of CSF1R^{+} myeloid cells within the allograft. At 30 d post-transplantation where allograft rejection was evident in tolerized *mHIF2−/−* recipients, both abundance of CSF1R^{+} myeloid cells and myeloid expression of CSF1R were reduced in the allografts of tolerized *mHIF2−/−* recipients compared to controls (Fig. 4*A*). To determine whether HIF-2α was required for generation of tolerogenic macrophages, we used flow cytometry to assess macrophage responses in tolerized allografts 7 d after transplantation. No difference in total number of CD11b^{+} myeloid cells was observed between allografts from tolerized *mHIF2+/+* and *mHIF2−/−* recipients (Fig. 4*B*), suggesting that HIF-2α was not required for myeloid cell trafficking to the allograft. However, monocyte to macrophage differentiation was impaired in tolerized *mHIF2−/−* recipients compared to controls as evidenced by increased expression of the monocytic marker, Ly6C, and reduced expression of macrophage markers, CD64, CD169, and MerTK (Fig. 4*C*). Tolerogenic macrophage marker, DC-SIGN, was also reduced and this was associated with reduced expression of CSF1R (Fig. 4*C*). Among CD11b^{+} myeloid cells expressing CSF1R, tolerogenic macrophages can be identified by low expression of Ly6C and Ly6G (11). Compared to controls, allografts from tolerized *mHIF2−/−* recipients contained less Ly6C^{lo} macrophages with a concomitant increase in immunogenic Ly6C^{hi} and Ly6G^{+} myeloid cells (Fig. 4*D*). Similar reductions were observed in CD206^{+} macrophages in tolerized *mHIF2−/−* recipients compared to controls (Fig. 4*E*), demonstrating that myeloid HIF-2α was required for the generation of tolerogenic macrophages during costimulatory blockade–induced cardiac transplantation tolerance.

Tolerogenic myeloid cells promote cardiac allograft survival in part through suppressing alloreactive T cells and promoting FoxP3^{+} T regulatory cells (23, 24). To examine lymphocytes during acute rejection or transplantation tolerance, we first rescaled and reclustered all lymphocyte subsets from both groups in our single-cell RNA sequencing dataset (Fig. 1 *A* and *B*), which led to the identification of seven transcriptionally distinct clusters (*SI Appendix*, Fig. S4 *A* and *B*). Using canonical marker genes, we identified one cluster of CD4^{+} T cells (*Cd3e* and *Cd4*), four clusters of CD8^{+} T cells (*Cd3e* and *Cd8a*), one cluster of CD8^{+} dendritic cells (*Cd8a, H2-Aa,* and *C1qa)*, and one cluster of natural killer (NK) cells (*Klra4* and *Gzma*) (*SI Appendix*, Fig. S4*C*). When we examined the proportion of lymphocyte clusters between acute rejection and tolerized cardiac allografts, we found that *S100a*4 CD8 T cells, *Mki67* CD8 T cells, and *Ptprc* CD8 T cells were increased within acute rejecting allografts, whereas tolerized allografts were characterized by increased abundance of *Ccr7* CD8 T cells, *Klra4* NK cells, and *Foxp3* CD4 T cells (*SI Appendix*, Fig. S4*D*). Pathway analyses of CD8 T cells during acute rejection revealed enrichment for activation, cytotoxicity, cytokine production, and glycolytic metabolism (*SI Appendix*, Fig. S4*E*). This was supported by increased expression of inflammatory effector genes, *Gzmb* and *Ifng* (*SI Appendix*, Fig. S4*F*). In contrast, apoptotic and cell death pathways were enriched in effector CD8 T cells during tolerance and this was associated with reduced

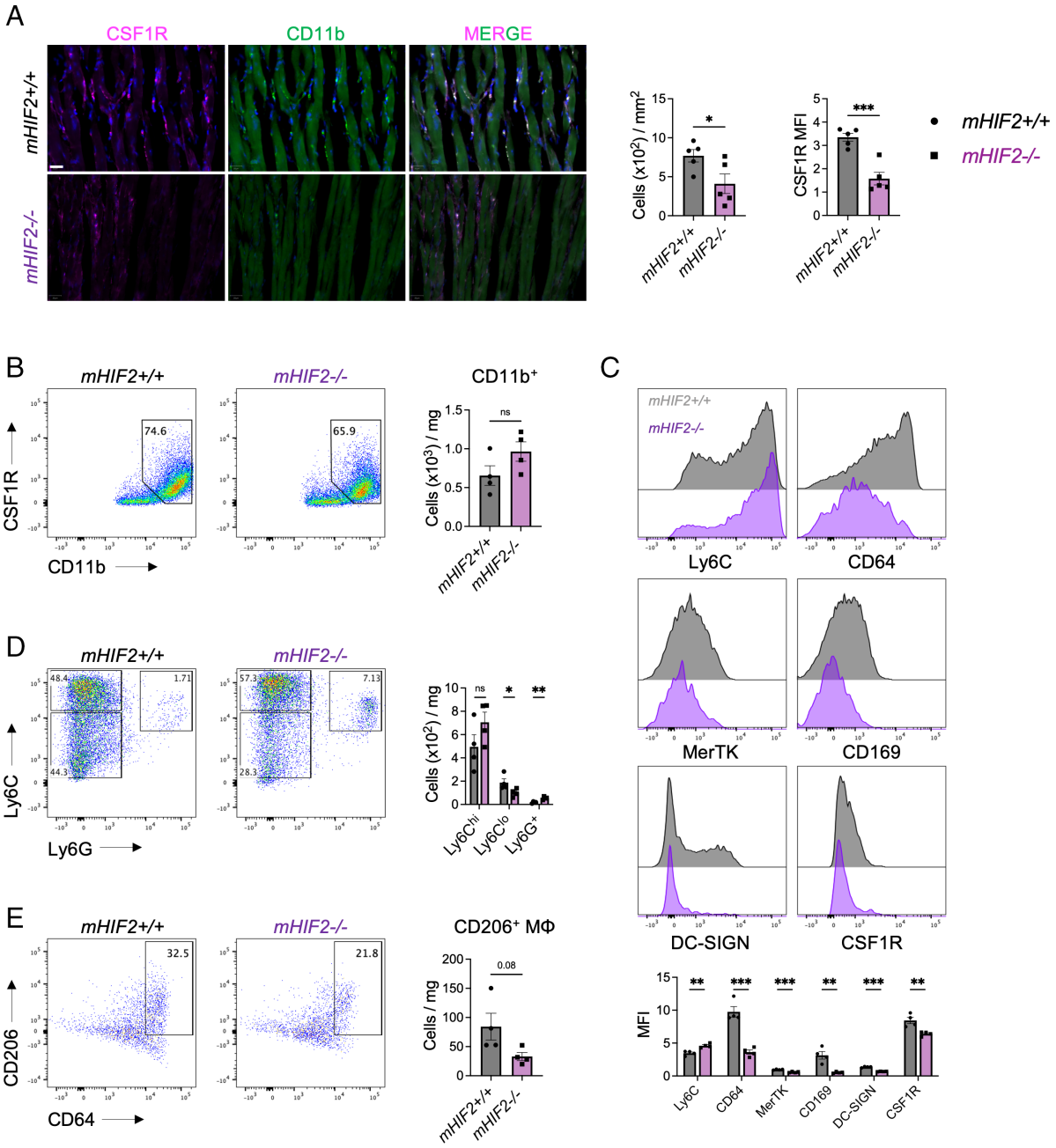

Fig. 4. Myeloid HIF-2α is required for accumulation of tolerogenic macrophages in the cardiac allograft. (*A*) Accumulation of myeloid cells expressing Colony Stimulating Factor 1 Receptor (CSF1R) in cardiac allografts from tolerized *mHIF2+/+* or *mHIF2−/−* recipients 30 d after transplantation with quantification of total abundance and mean fluorescent intensity (MFI) of CSF1R. $n = 5$ mice/group pooled from two independent experiments. $^{*}P < 0.05$ and $^{***}P < 0.001$ by the two-tailed, unpaired *t* test. (Scale bar, 20 μm.) (*B*) Total abundance of $CD11b^{+}$ myeloid cells in cardiac allografts from tolerized *mHIF2+/+* or *mHIF2−/−* recipients 7 d after transplantation. $n = 4$ mice/group pooled from two independent experiments. ns, not significant by the two-tailed, unpaired *t* test. (*C*) Expression of monocyte and macrophage markers on the $CD11b^{+}CSF1R^{+}$ myeloid cell gate in panel (*B*). $n = 4$ mice/group pooled from two independent experiments. $^{**}P < 0.01$ and $^{***}P < 0.001$ by the two-tailed, unpaired *t* test. (*D*) Total abundance of $Ly6C^{hi}$, $Ly6C^{lo}$, and $Ly6G^{+}$ cells among the $CD11b^{+}CSF1R^{+}$ myeloid cell gate in panel (*B*). $n = 4$ mice/group pooled from two independent experiments. $^{*}P < 0.05$ and $^{**}P < 0.01$ by the two-tailed, unpaired *t* test. (*E*) Total abundance of $CD206^{+}$ macrophages among the $Ly6C^{lo}Ly6G^{-}$ myeloid cell gate in panel (*D*). $n = 4$ mice/group pooled from two independent experiments. $P = 0.08$ by the two-tailed, unpaired *t* test.

expression of *Gzmb* and *Ifng* (*SI Appendix*, Fig. S4 *E* and *F*). Interestingly, the *Foxp3* CD4 T cell cluster exhibited context-dependent transcriptional responses. While *Foxp3* CD4 T cells were enriched for glycolytic metabolism and expressed high levels of *Gzmb* and *Ifng* during acute rejection, these cells shifted toward oxidative metabolism and expression of anti-inflammatory *Il10* during transplantation tolerance (*SI Appendix*, Fig. S4 *E* and *F*), which was associated with increased *Foxp3* expression (*SI Appendix*, Fig. S4*G*). Similar to myeloid cells, these data support distinct transcriptional reprogramming of lymphocytes during transplantation tolerance compared to acute rejection.

Given that HIF-2α was required for the generation of tolerogenic macrophages, we sought to corroborate the functional consequences by measuring changes in $CD4^{+}$ or $CD8^{+}$ T cells within the allograft and spleen. While no difference was observed in total number of allograft-associated $CD8^{+}$ T cells, $CD4^{+}$ T cell abundance was increased in allografts from tolerized *mHIF2−/−* recipients compared to controls (*SI Appendix*, Fig. S5*A*). When we assessed $CD4^{+}$ T cell activation status, we found increased numbers of effector $CD4^{+}$ T cells (*SI Appendix*, Fig. S5*B*), with a concomitant decrease in $FoxP3^{+}$ T regulatory cells in allografts from tolerized *mHIF2−/−* recipients compared to controls (*SI Appendix*, Fig. S5*C*). Similar reductions in

FoxP3$^+$ T regulatory cells were also observed in the allografts of tolerized *Ccr2*−/− recipients (*SI Appendix*, Fig. S2 *H* and *I*). Despite no difference in total numbers of allograft-associated CD8$^+$ T cells or effector CD8$^+$ T cells (*SI Appendix*, Fig. S5 *A* and *D*), we found that CD8$^+$ T cell exhaustion was impaired in allografts from tolerized *mHIF2*−/− recipients compared to controls as measured by reduced CD8$^+$ T cell expression of inhibitory receptors, PD-1 and LAG3 (*SI Appendix*, Fig. S5*E*). In contrast to the changes we observed in the allograft, no differences were observed in total number of T cells (*SI Appendix*, Fig. S5*F*), effector CD4$^+$ T cells, FoxP3$^+$ T regulatory cells, effector CD8$^+$ T cells or exhausted CD8$^+$ T cells (*SI Appendix*, Fig. S5 *G*–*J*) in the spleen from tolerized *mHIF2*−/− recipients compared to controls. However, peripheral alloreactivity was still evident in tolerized *mHIF2*−/− recipients compared to controls as measured by increased serum levels of donor-specific antibodies (*SI Appendix*, Fig. S5*K*), which also mediate transplant rejection along with the alloreactive B cells that produce them (25). Taken together, these data indicate that HIF-2α directs myeloid cell function that leads to suppression of alloreactive immune responses and promotion of allograft-protective FoxP3$^+$ T regulatory cells.

Since treatment of heart transplant recipients with a CCR2 antagonist revealed monocyte mobilization from the spleen during transplantation tolerance, we next examined how HIF-2α affected splenic myeloid cell responses. At 7 d after transplantation, neutrophil abundance was increased in the spleens from tolerized *mHIF2*−/− recipients compared to controls (Fig. 5*A*). In contrast, no difference in macrophage or Ly6C^{hi} monocyte abundance was observed between tolerized *mHIF2*+/+ and *mHIF2*−/− recipients (Fig. 5 *B* and *C*). Given that HIF-2α promoted tolerogenic macrophage expression of CSF1R in cardiac allografts, we also explored myeloid cell expression of CSF1R in the spleen. While no difference in CSF1R levels was observed on splenic neutrophils or macrophages between tolerized *mHIF2*+/+ and *mHIF2*−/− recipients (Fig. 5 *D* and *E*), CSF1R was reduced on Ly6C^{hi} monocytes in the spleens from tolerized *mHIF2*−/− recipients compared to controls (Fig. 5*F*). Combined with our earlier pseudotime observation that Ly6C^{hi} monocytes increase *Csf1r* expression on their path to becoming tolerogenic macrophages, this suggests that HIF-2α activation in splenic monocytes plays a key role in this differentiation process.

To better understand the relationship between HIF-2α and CSF1R in the absence of any confounding effect of surgically induced inflammation, we modeled donor antigen exposure during transplantation tolerance by injecting mice with a single dose of costimulatory blockade and donor splenocytes (CoB/DSC) and isolated recipient splenic monocytes 72 h later (Fig. 6*A*). While CoB/DSC treatment did not affect splenic neutrophil abundance (Fig. 6*B*), Ly6C^{hi} monocyte abundance was increased in the spleens of mice treated with CoB/DSC compared to controls (Fig. 6*C*). This effect required HIF-2α as the CoB/DSC-dependent increase in splenic monocytes was abrogated in *mHIF2*−/− mice (Fig. 6*C*). HIF-2α was also required for the differentiation of Ly6C^{hi} monocytes into Ly6C^{lo} macrophages and suppression of T cell proliferation (*SI Appendix*, Fig. S6). As a complementary approach, we also isolated monocytes from mice expressing myeloid-specific, prolyl hydroxylation-resistant HIF-2α (*mHIF2*^{LSL}), leading to constitutively higher levels of HIF-2α in monocytes and macrophages (26, 27). Compared to controls, monocytes from *mHIF2*^{LSL} exhibited

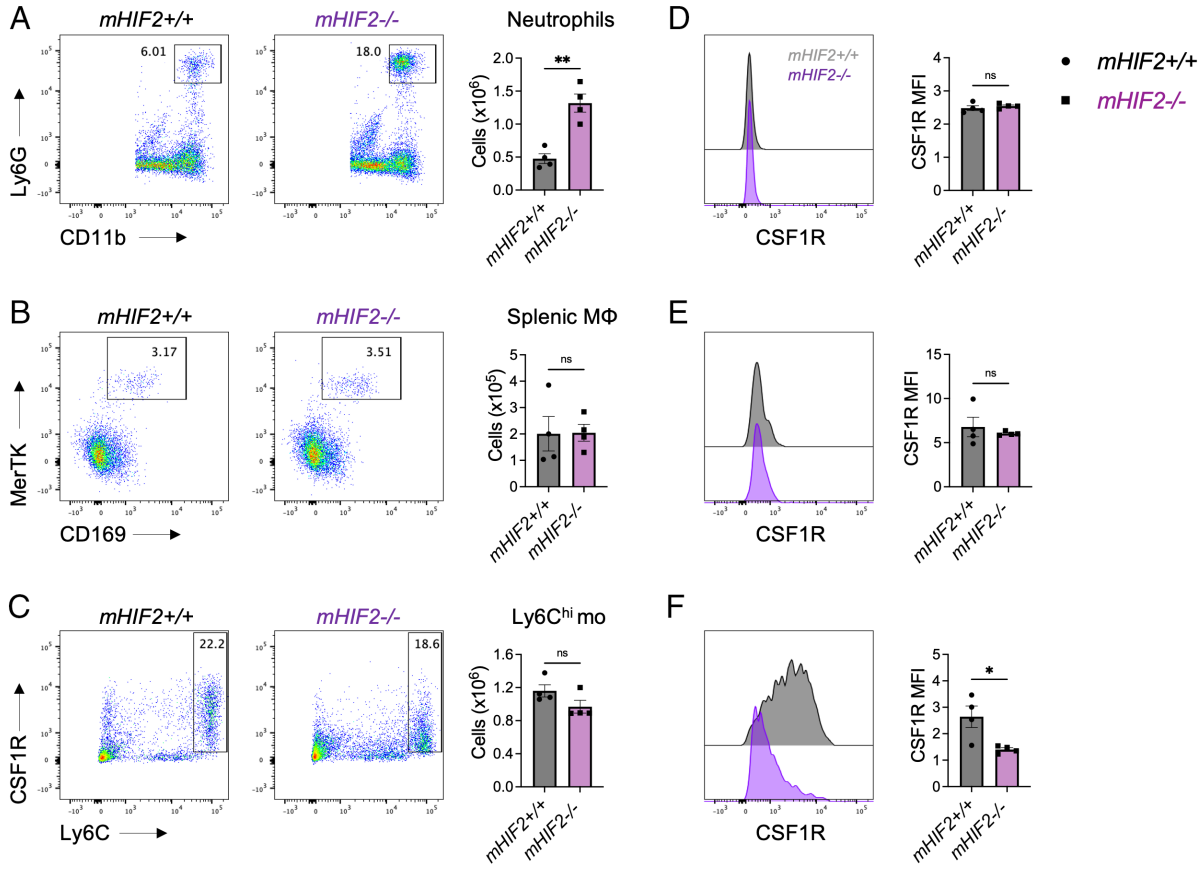

Fig. 5. Myeloid HIF-2α is required for tolerogenic monocyte expression of CSF1R in the spleen. Total abundance of (*A*) neutrophils, (*B*) macrophages, and (*C*) monocytes in spleens from tolerized *mHIF2*+/+ or *mHIF2*−/− recipients 7 d after heart transplantation. $n = 4$ mice/group pooled from two independent experiments. $^{**}P < 0.01$ by the two-tailed, unpaired *t* test. Expression of Colony Stimulating Factor 1 Receptor (CSF1R) on (*D*) neutrophils, (*E*) macrophages, and (*F*) monocytes in spleens from tolerized *mHIF2*+/+ or *mHIF2*−/− recipients 7 d after heart transplantation with quantification of mean fluorescent intensity (MFI) of CSF1R. $n = 4$ mice/group pooled from two independent experiments. $^{*}P < 0.05$ by the two-tailed, unpaired *t* test.

even greater suppression of T cell proliferation (*SI Appendix*, Fig. S6). Importantly, CoB/DSC treatment led to increased expression of HIF-2α in splenic monocytes from *mHIF2*+/+ mice (Fig. 6*D*), and this was associated with increased expression of CSF1R in splenic monocytes from *mHIF2*+/+ mice but not *mHIF2*−/− mice (Fig. 6*E*). Since infusion of CoB/DSC was sufficient to promote HIF-2α in splenic monocytes, we further explored whether direct interaction between myeloid cells and CoB/DSC promoted HIF-2α expression by coculturing bone marrow–derived macrophages (BMDMs) with CoB/DSC in vitro. Compared to untreated BMDMs, HIF-2α levels were increased in BMDMs cocultured with CoB/DSC, which was associated with increased expression of CSF1R and tolerogenic macrophage marker, CD206 (*SI Appendix*, Fig. S7). Together, these data suggest that myeloid cells can be directly reprogrammed by CoB/DSC, which occurs independent of CD36.

Given the positive association between HIF-2α and CSF1R in myeloid cells after CoB/DSC treatment, we hypothesized that *Csf1r* was a direct transcriptional target of HIF-2α. Monocyte expression of *Csf1r* is regulated in part by the myeloid-specific *fms*-intronic regulatory element (FIRE) enhancer (28), and we first established a hypothetical relationship between HIF-2α and *Csf1r* by identifying conserved HIF binding sites, known as hypoxia response elements (HRE) (29), within the *Csf1r* promotor (Fig. 6*F*). Next, we performed chromatin immunoprecipitation on magnetically selected splenic monocytes after CoB/DSC treatment to determine whether HIF-2α directly bound to the *Csf1r* promotor. We found that increased HIF-2α binding to the *Csf1r* promotor was evident in monocytes from the spleens of *mHIF2*+/+ mice but not *mHIF2*−/− mice after CoB/DSC treatment (Fig. 6*G*), demonstrating a direct relationship between HIF-2α and CSF1R in myeloid cells.

Finally, to test the therapeutic potential of our findings, we treated mice with roxadustat (30), a prolyl hydroxylase (PHD) inhibitor that stabilizes HIF-2α and increases expression of HIF-2α target genes (Fig. 7*A*). To enhance targeting of roxadustat to the myeloid compartment and limit adverse effects associated with the drug (31), we encapsulated roxadustat within poly(ethylene glycol)-b-poly(propylene sulfide) (PEG-PPS) micelles (Fig. 7*B*). PEG-PPS nanocarriers have been previously employed in tolerogenic strategies (32), primarily due to their selective uptake by monocytes, macrophages, and dendritic cells within the spleen and other organs (33). Treatment of mice with roxadustat-loaded micelles (RoxMC)increased splenic monocyte HIF-2α protein to levels seen with mice treated with roxadustat alone (Fig. 7*C*), and this was associated with increased expression of CSF1R on monocytes compared to vehicle controls (Fig. 7*D*). Similar increases in HIF-2α protein was also observed in vitro after treatment of BMDMs with RoxMC or roxadustat alone (*SI Appendix*, Fig. S8). Consistent with previous reports (34, 35), treatment of mice with roxadustat alone increased plasma levels of erythropoietin (Fig. 7*E*). However, this effect was blunted in mice treated with RoxMC (Fig. 7*E*), reflecting enhanced targeting of roxadustat to the myeloid compartment. To test whether RoxMC could enhance transplantation tolerance, we treated mice with unloaded control micelles or RoxMC in combination with a dosing strategy of costimulatory blockade antibody that was previously shown to lead to cardiac allograft rejection between 20 and 40 d after transplantation (36) (Fig. 7*F*). In line with previous findings, cardiac allograft rejection was evident in mice treated with control micelles and costimulatory blockade beginning 23 d after transplantation (Fig. 7*G*). In contrast, cardiac allograft survival was significantly enhanced in mice treated with RoxMC and costimulatory blockade (Fig. 7*G*). Furthermore, recipient mice treated with RoxMC exhibited reduced allograft vasculopathy (Fig. 7*H*) and serum levels of donor-specific antibodies (Fig. 7*I*) compared to controls. Enhanced allograft survival was also observed in $mHIF2^{LSL}$ mice only treated with costimulatory blockade (Fig. 7*G*). In contrast, RoxMC treatment had no effect on allograft survival in *mHIF2*−/− recipients (*SI Appendix*, Fig. S9) demonstrating that increased HIF-2α levels in myeloid cells alone were sufficient to induce long-term transplantation tolerance. Taken together, these data identify RoxMC as a therapeutic strategy to increase HIF-2α activation in myeloid cells and promote transplantation tolerance.

Discussion

Our data reveal a role for HIF-2α in transplantation tolerance. According to our working model (*SI Appendix*, Fig. S10), heart transplantation with costimulatory blockade activates HIF-2α and transcription of its target gene, *Csf1r*, in splenic monocytes. Following CCR2-dependent recruitment of these monocytes to the allograft, CSF1-CSF1R signaling promotes monocyte differentiation into tolerogenic macrophages. Within the allograft, these macrophages maintain a tolerogenic state by suppressing alloreactive T cell responses and inducing allograft protective $FoxP3^+$ T regulatory cells. Administration of the HIF activator, roxadustat, within micelles for selective targeting to myeloid cells, increased monocyte expression of CSF1R and enhanced cardiac allograft survival. These findings establish the foundation to investigate myeloid HIF-2α activation as a target for transplantation tolerance in humans.

While HIF signaling has been previously reported to confer allograft protection, this was in the perioperative setting of allograft ischemia or reperfusion injury and limited to HIF-1α activation (37, 38). Comparatively less is known about HIF-2α in transplantation, so our findings establish a timely connection between HIF-2α and transplantation tolerance. The tolerogenic role for HIF-2α in myeloid cells was unexpected since HIF-2α has been implicated in the inflammatory activation of macrophages after acute cardiac injury (27) and endotoxemia (13). However, emerging evidence in the absence of tolerogenic stimuli also supports our findings for an allograft protective role for HIF-2α. In human heart failure, increased expression of PHD3, which selectively antagonizes HIF-2α over HIF-1α (39), was associated with reduced HIF-2α expression (40). Similarly, increased levels of PHD3 were associated with the onset of fibrosis in rejecting human cardiac allografts (41), providing indirect evidence for HIF-2α in allograft protection. In mice, selective overexpression of HIF-2α in endothelial cells promoted allograft survival in a nonvascularized tracheal transplantation model (42), and selective overexpression of both HIF-1α and HIF-2α in myeloid cells prolonged cardiac allograft survival in the absence of immunosuppression (43). We observed variable *Hif1* and *Hif2* gene expression among different tolerogenic myeloid cells, supporting further exploration of both HIF-1α and HIF-2α in transplantation tolerance.

Despite a clear role for HIF-2α in transplantation tolerance, the molecular mechanisms leading to its activation within this setting remain incomplete. Tissue hypoxia during cold organ storage and transport increases HIF-1α levels that are sustained for hours to weeks following transplantation and reperfusion in humans (37, 41). After reperfusion of kidney allografts in rats, pimonidazole staining revealed that this sustained activation of HIF-1α occurs in the absence of allograft hypoxia (44). Compared to HIF-1α, HIF-2α is less susceptible to normoxic degradation (45), suggesting that allograft ischemia-reperfusion may also trigger HIF-2α activation in allograft infiltrating recipient monocytes that remains elevated during their differentiation into tolergenic macrophages. We also found evidence for hypoxia-independent activation of HIF-2α during transplantation tolerance, which occurred through direct interaction of myeloid cells with

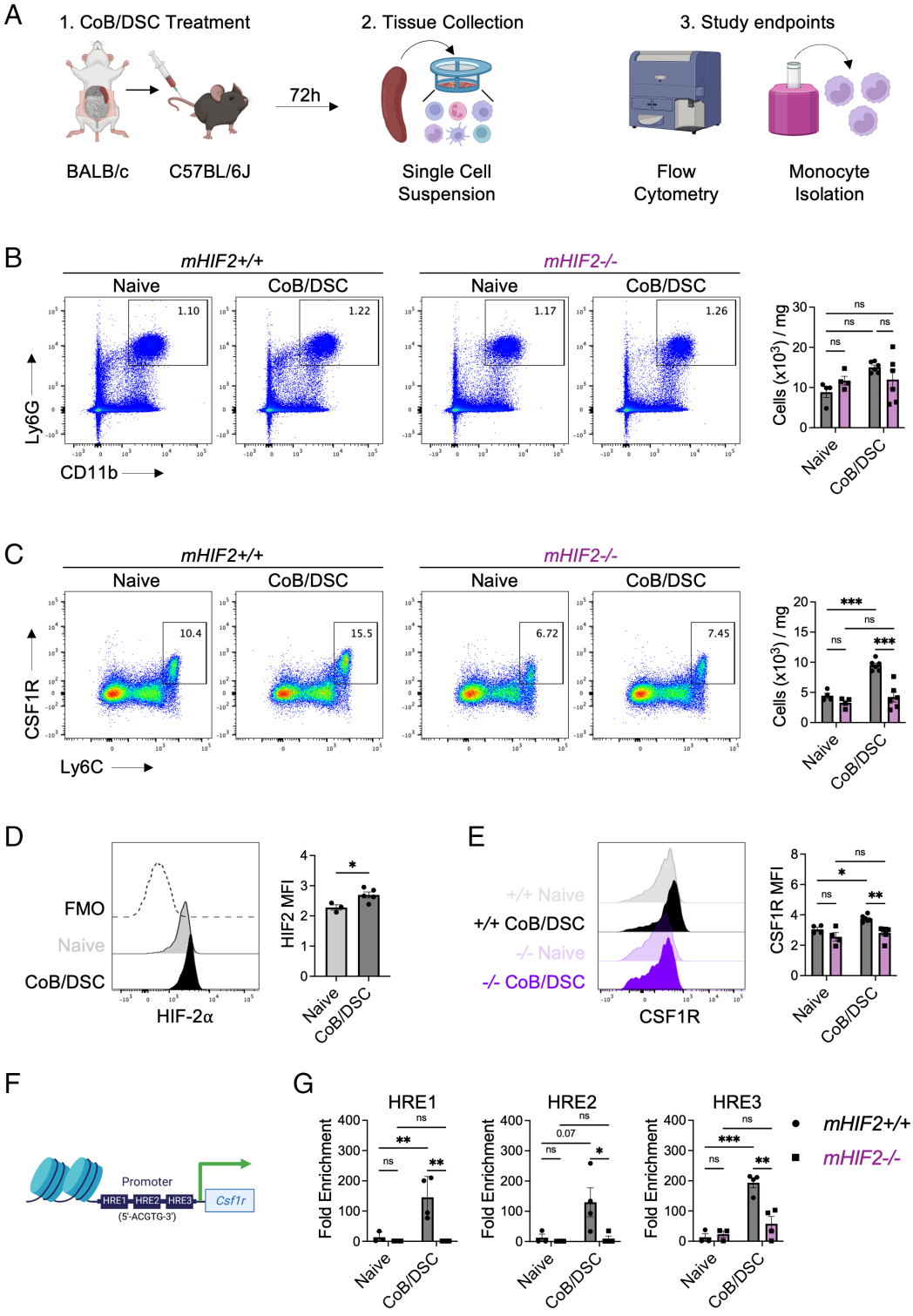

Fig. 6. *Csf1r* is a direct transcriptional target of HIF-2α in tolerogenic monocytes within the spleen. (*A*) Experimental design for treating mice with costimulatory blockade (CoB) and donor spleen cells (DSC) prior to collection of spleens from recipient mice and study endpoints. Total abundance of (*B*) neutrophils and (*C*) Ly6C^{hi} monocytes in the spleens of *mHIF2+/+* or *mHIF2−/−* mice 72 h after CoB/DSC treatment. n = 5 to 6 mice/group pooled from two independent experiments. ***P < 0.001 by two-way ANOVA followed by Tukey's test. (*D*) Expression of HIF-2α in splenic Ly6C^{hi} monocytes 72 h after CoB/DSC treatment. n = 3 to 5 mice/group pooled from two independent experiments. The dashed line represents fluorescent minus one (FMO) staining control. *P < 0.05 by the two-tailed, unpaired t test. (*E*) Expression of Colony Stimulating Factor 1 Receptor (CSF1R) on Ly6C^{hi} monocytes in the spleens of *mHIF2+/+* or *mHIF2−/−* mice 72 h after CoB/DSC treatment. (*F*) Schematic of hypoxia response elements (HRE) on the *Csf1r* promotor region. (*G*) Chromatin immunoprecipitation for HIF-2α on the *Csf1r* promotor in splenic Ly6C^{hi} monocytes from *mHIF2+/+* or *mHIF2−/−* mice 72 h after CoB/DSC treatment. n = 3 to 4 mice/group pooled from two independent experiments. *P < 0.05, **P < 0.01, and ***P < 0.001 by two-way ANOVA followed by Tukey's test.

alloantigen during costimulatory blockade. Following treatment of mice or macrophages with donor-derived cells and costimulatory blockade, HIF-2α levels were increased leading to enhanced expression of CSF1R and CD206. Transplantation tolerance and HIF-2α activation were unaffected by genetic deletion of *Cd36*, necessitating additional studies to elucidate the signals for HIF-2α activation during transplantation tolerance.

Although a tolerogenic role for CCR2^{+} monocytes was somewhat surprising, given their well-characterized role during ischemia–reperfusion injury (46–48) or antibody-mediated rejection (49), monocytes have emerged as protagonists of costimulatory blockade–induced transplantation tolerance. Previous work has shown that monocytes expressing both Ly6C and Ly6G were mobilized from the bone marrow and recruited to the allograft to establish tolerance (8). During costimulatory blockade, we observed increased splenic CCR2^{+} monocytes within the spleen. Treatment of mice with a CCR2 antagonist during costimulatory blockade further increased abundance of CCR2^{+} monocytes within the spleen revealing that the spleen also serves as a reservoir for monocytes during transplantation tolerance. Additional studies are needed to determine whether monocytes derived from bone marrow or spleen have distinct or overlapping functions during transplantation tolerance. The presence of activated T cells within the allograft but not the spleen highlights the importance of

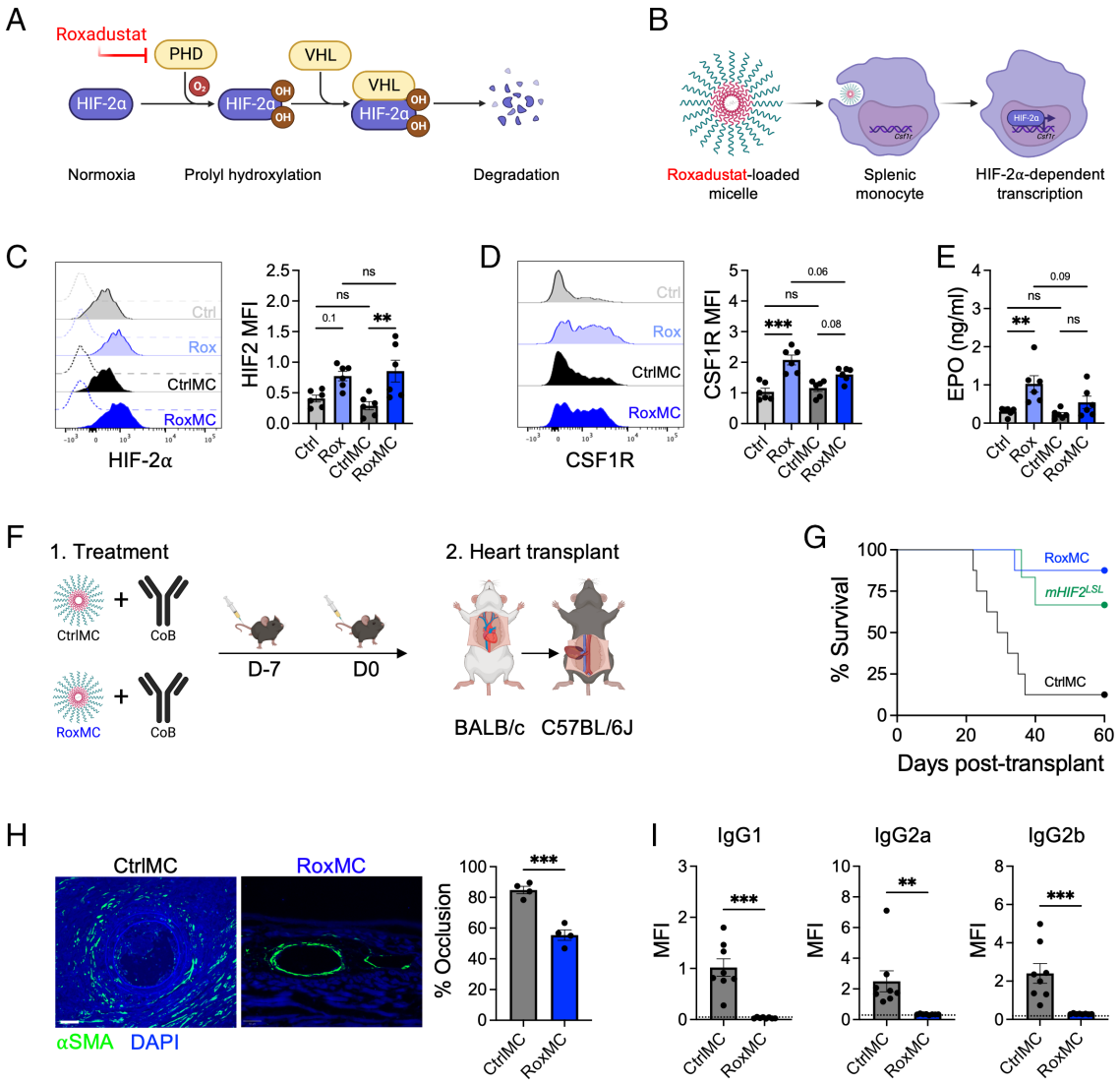

Fig. 7. Therapeutic stabilization of HIF-2α in myeloid cells promotes cardiac allograft survival. (*A*) Schematic of the roxadustat mechanism of action to stabilize HIF-2α. Roxadustat inhibits prolyl hydrolase (PHD) mediated hydroxylation of HIF-2α to prevent its degradation by Von Hippel–Lindau tumor suppressor (VHL). (*B*) Schematic of targeting roxadustat to splenic monocytes using roxadustat-loaded poly(ethylene glycol)-b-poly(propylene sulfide) (PEG-PPS) micelles. (*C*) Expression of HIF-2α in splenic monocytes following treatment of mice with roxadustat alone (Rox), roxadustat-loaded micelles (RoxMC), or vehicle controls (Ctrl/MC). n = 6 mice/group pooled from two independent experiments. $^{**}P < 0.01$ by two-way ANOVA followed by Tukey's test. (*D*) Expression of Colony Stimulating Factor 1 Receptor (CSF1R) on splenic monocytes following treatment of mice with Rox, RoxMC, or CtrlMC. n = 6 mice/group pooled from two independent experiments. $^{***}P < 0.001$ by two-way ANOVA followed by Tukey's test. (*E*) Plasma levels of erythropoietin (EPO) following treatment of mice with Rox, RoxMC, or CtrlMC. n = 6 mice/group pooled from two independent experiments. $^{**}P < 0.01$ by two-way ANOVA followed by Tukey's test. (*F*) Experimental design for combined treatment of mice with RoxMC and costimulatory blockade (CoB) during heart transplantation. (*G*) Cardiac allograft survival in C57BL/6J recipients treated with CoB and RoxMC or CtrlMC. Alternatively, cardiac allograft survival was assessed in mice with myeloid-specific, prolyl hydroxylation-resistant HIF-2α (*mHIF2*^{LSL}) treated with CoB alone. n = 6 to 8 mice/group pooled from three independent experiments. $^{*}P < 0.05$ by the log-rank (Mantel–Cox) test compared to the CtrlMC group. (*H*) Expression of α-Smooth Muscle Actin (SMA) in cardiac allografts from CtrlMC- or RoxMC-treated recipients 60 d after transplantation with quantification of percent vessel occlusion. n = 4 mice/group pooled from two independent experiments. $^{***}P < 0.001$ by the two-tailed, unpaired t test. (Scale bar, 50 μm.) (*I*) Donor-specific antibodies in serum of CtrlMC- or RoxMC-treated recipients 60 d after heart transplantation. The dashed line represents no serum staining control. n = 8 mice/group pooled from two independent experiments. $^{**}P < 0.01$ by the two-tailed, unpaired t test.

CCR2-dependent splenic monocyte mobilization to the allograft followed by differentiation into tolerogenic macrophages. These events are also important in dampening allograft infiltration of neutrophils, which are associated with accelerated rejection of cardiac allografts in mice and humans (50–52). Further evidence for the necessity of monocyte-derived macrophages in transplantation tolerance comes from the observation that donor-derived myeloid cells are completely lost from the allograft within 1 to 2 wk post-transplant (53). This challenges the binary resident vs. recruited macrophage paradigm during sterile inflammation that resident macrophages are protective, while recruited monocyte-derived macrophages are detrimental to normal tissue function (54, 55). Compared to acute rejection, recruited monocyte-derived macrophages adapted a homeostatic transcriptional fate demonstrating that recruited monocyte-derived macrophages can be reprogramed toward tissue protection.

Transplantation tolerance after costimulatory blockade requires CSF1 signaling through its cognate receptor CSF1R to promote monocyte differentiation into tolerogenic DC-SIGN^{+} macrophages (11). Here, we identified a molecular link to CSF1R through the transcription factor HIF-2α. Loss of HIF-2α was associated with reduced expression of CSF1R on splenic monocytes during costimulatory blockade, which led to impaired accumulation of CD206^{+} tolerogenic macrophages within the allograft. While a previous study reported reduced CSF1R levels in BMDMs from *mHIF2*−/− mice (13), we established a definitive link between HIF-2α and

CSF1R through HIF-2α binding directly to HREs on the *Csf1r* promotor. HIF-dependent regulation of *Csf1r* expression has also been observed in tumor cells, where acriflavine, an inhibitor of both HIF-1α and HIF-2α, blocked hypoxia-induced *Csf1r* expression (56). The link between HIF-2α and CSF1R signaling shared in the setting of organ transplantation and cancer raises the possibility that mechanistic insight into transplantation tolerance may be gained from the immune reprogramming that occurs within the tumor microenvironment. For example, $CD206^+$ tumor-associated macrophages support proliferation of oral squamous cell carcinoma (57), and loss of HIF-2α in tumor-associated macrophages blunts colitis-associated cancer (13). Similar parallels are likely to exist for immune tolerance between organ transplantation and pregnancy, where tolerogenic $CD206^+$ macrophages expressing DC-SIGN accumulate at the maternal–fetal interface (58). Additional studies are needed to resolve the role of myeloid cell expression of HIF-2α and the mechanisms governing immune tolerance among organ transplantation, cancer, and pregnancy (59, 60).

While we uncovered a role for HIF-2α in the development of tolerogenic macrophages, it also likely plays an important role in the function of these cells. For example, HIF-1α and HIF-2α transcriptionally regulate adenosine receptors (Adora) (61, 62), which are activated by extracellular adenosine to attenuate inflammatory responses and confer tissue protection. Adora2a levels are increased in peripheral blood mononuclear cells after heart transplantation in humans (63), and pharmacologic enhancement of adenosine levels in rat cardiac allografts blunts infiltration of inflammatory cells into the allograft (64, 65). Adenosine signaling also promotes the development of $FoxP3^+$ T regulatory cells (66), suggesting that boosting HIF-adenosine signaling may promote transplantation tolerance. Amphiregulin (Areg) is another HIF-2α target gene that confers cardioprotection after ischemia-reperfusion injury (67). Our single-cell transcriptomic analyses of cardiac allografts revealed that $FoxP3^+$ T regulatory cells were enriched for *Areg* expression. Production of Areg by $FoxP3^+$ T regulatory cells is necessary to suppress inflammation (68, 69), and *Hif2*-deficient $FoxP3^+$ T regulatory cells are functionally defective (70). HIF-2α also promotes transcription-independent induction of the Areg receptor, epidermal growth factor receptor 1 in cardiomyocytes (71), supporting further exploration of the role of HIF-2α in tolerogenic macrophages and $FoxP3^+$ T regulatory cells as well as cellular cross talk during transplantation tolerance.

In a therapeutic context, our findings suggest that combined HIF-2α activation and costimulatory blockade may promote long-term tolerance and limit the need for chronic immunosuppression. Several small molecule inhibitors that target PHDs and stabilize HIF-2α are already in clinical use, including roxadustat (30, 72). Previous studies administering a single dose of roxadustat to donor animals prior to transplantation of kidney (73) or abdominal aorta (74) ameliorated vasculopathy and improved allograft survival in recipient animals. Off-target systemic effects remain an obstacle for roxadustat clinical approval, so we packaged roxadustat into micelles to selectively target roxadustat to phagocytes, including splenic monocytes. Delivery of RoxMC inhibited alloreactive responses and increased allograft survival, supporting the notion that HIF activation by PHD inhibitors may represent a strategy to promote long-term allograft survival. Mice with selective overexpression of HIF-2α in myeloid cells phenocopied the enhanced allograft survival of roxadustat-treated animals, demonstrating that HIF-2α activation alone was sufficient to achieve therapeutic benefit. HIF-2α is positively regulated by mTOR (75), which is a target of current immunosuppressive drug, rapamycin. Transient treatment with rapamycin does not hinder induction of experimental transplantation tolerance in rodents or nonhuman primates (12, 76, 77). However, rapamycin treatment or genetic deletion of mTOR has also been shown to impair myeloid-derived suppressor cell differentiation and function in allografts and tumors (78–80), necessitating additional studies on the interaction between roxadustat and current immunosuppressive drugs.

In conclusion, our findings reveal that transplantation tolerance requires HIF-2α signaling in monocytes to promote their differentiation into tolerogenic macrophages, which was mediated in part by direct transcriptional regulation of *Csf1r*. The identified role for HIF-2α in transplantation tolerance has implications in other settings of immune tolerance, including pregnancy and cancer, and supports its therapeutic activation in the setting of heart transplantation to promote long-term survival in humans.

Methods (Extended Methods in *SI Appendix*)

Mice. Mice with myeloid-specific overexpression of HIF-2α were generously provided by Yatrik Shah [University of Michigan, Ann Arbor, MI; (81)].

Heterotopic Heart Transplantation. Mice of B6 background were subjected to full MHC-mismatch abdominal heart transplantation as previously described (82, 83) in collaboration with Northwestern's Microsurgery and Preclinical Research Core.

Transplantation Tolerance Induction. For tolerance induction, mice received intravenous infusions of anti-CD40L antibody (500 μg per mouse) and donor BALB/c splenocytes (2×10^7 cells) on day 0 prior to transplantation, followed by intraperitoneal injections of anti-CD40L (500 μg per mouse) on days 7 and 14 posttransplantation as previously described (84, 85). For experiments assessing the effect of roxadustat on allograft survival, mice received intraperitoneal injections of anti-CD40L antibody (250 μg per mouse) on days −7 and 0 for allograft rejection between days 20 and 40 posttransplantation (36).

Data, Materials, and Software Availability. Mouse transcriptomics data are accessible at NCBI GEO (GSE262851) (86). All other data are included in the manuscript or *SI Appendix*.

ACKNOWLEDGMENTS. This work was supported by the American Heart Association (grant CDA34110032 to M.D.) and the NIH (grant R01HL139812 to E.B.T.). Publication of this research was supported by the Sidney and Bess Eisenberg Memorial Fund.

Author affiliations: [a]Department of Pathology, Feinberg School of Medicine, Northwestern University, Chicago, IL 60611; [b]Department of Anesthesiology, Critical Care and Pain Medicine, University of Texas Health Science Center, Houston, TX 77030; [c]Department of Biomedical Engineering, Northwestern University, Evanston, IL 60208; [d]Department of Surgery, Comprehensive Transplant Center, Northwestern University, Chicago, IL 60611; and [e]Division of Nephrology and Hypertension, Feinberg School of Medicine, Northwestern University, Chicago, IL 60611

1. S. K. Bhagra, S. Pettit, J. Parameshwar, Cardiac transplantation: Indications, eligibility and current outcomes. *Heart* **105**, 252–260 (2019).
2. M. A. A. Jansen, H. G. Otten, R. A. de Weger, M. M. H. Huibers, Immunological and fibrotic mechanisms in cardiac allograft vasculopathy. *Transplantation* **99**, 2467–2475 (2015).
3. H. J. Eisen *et al.*, Everolimus for the prevention of allograft rejection and vasculopathy in cardiac-transplant recipients. *N Engl. J. Med.* **349**, 847–858 (2003).
4. J. D. Morrisett *et al.*, Effects of sirolimus on plasma lipids, lipoprotein levels, and fatty acid metabolism in renal transplant patients. *J. Lipid Res.* **43**, 1170–1180 (2002).
5. J. R. Leventhal, J. M. Mathew, Outstanding questions in transplantation: Tolerance. *Am. J. Transpl.* **20**, 348–354 (2020).
6. J. Ochando, P. Conde, A. Utrero-Rico, E. Paz-Artal, Tolerogenic role of myeloid suppressor cells in organ transplantation. *Front. Immunol.* **10**, 374 (2019).
7. X. Jiang *et al.*, Cardiac allograft acceptance induced by blockade of CD40-CD40L costimulation is dependent on $CD4^+CD25^+$ regulatory T cells. *Surgery* **149**, 336–346 (2011).
8. M. R. Garcia *et al.*, Monocytic suppressive cells mediate cardiovascular transplantation tolerance in mice. *J. Clin. Invest.* **120**, 2486–2496 (2010).

9. A.-S. Dugast *et al.*, Myeloid-derived suppressor cells accumulate in kidney allograft tolerance and specifically suppress effector T cell expansion1. *J. Immunol.* **180**, 7898–7906 (2008).
10. W. Zhang, S. Liang, J. Wu, A. Horuzsko, Human inhibitory receptor immunoglobulin-like transcript 2 amplifies CD11b+Gr1+ myeloid-derived suppressor cells that promote long-term survival of allografts. *Transplantation* **86**, 1125–1134 (2008).
11. P. Conde *et al.*, DC-SIGN$^+$ macrophages control the induction of transplantation tolerance. *Immunity* **42**, 1143–1158 (2015).
12. M. S. Braza *et al.*, Inhibiting inflammation with myeloid cell-specific nanobiologics promotes organ transplant acceptance. *Immunity* **49**, 819–828.e816 (2018).
13. H. Z. Imtiyaz *et al.*, Hypoxia-inducible factor 2alpha regulates macrophage function in mouse models of acute and tumor inflammation. *J. Clin. Invest.* **120**, 2699–2714 (2010).
14. M. Lamas Bervejillo *et al.*, A FABP4-PPARγ signaling axis regulates human monocyte responses to electrophilic fatty acid nitroalkenes. *Redox Biol.* **29**, 101376 (2020).
15. I. Hilgendorf *et al.*, Ly-6Chigh monocytes depend on Nr4a1 to balance both inflammatory and reparative phases in the infarcted myocardium. *Circ. Res.* **114**, 1611–1622 (2014).
16. C. Trapnell *et al.*, The dynamics and regulators of cell fate decisions are revealed by pseudotemporal ordering of single cells. *Nat. Biotechnol.* **32**, 381–386 (2014).
17. K. J. Lavine *et al.*, Distinct macrophage lineages contribute to disparate patterns of cardiac recovery and remodeling in the neonatal and adult heart. *Proc. Natl. Acad. Sci. U.S.A.* **111**, 16029–16034 (2014).
18. M. DeBerge *et al.*, MerTK cleavage on resident cardiac macrophages compromises repair after myocardial ischemia reperfusion injury. *Circ. Res.* **121**, 930–940 (2017).
19. F. K. Swirski *et al.*, Identification of splenic reservoir monocytes and their deployment to inflammatory sites. *Science* **325**, 612–616 (2009).
20. N. Lin, M. C. Simon, Hypoxia-inducible factors: Key regulators of myeloid cells during inflammation. *J. Clin. Invest.* **126**, 3661–3671 (2016).
21. M. Liao *et al.*, HIF-2α-induced upregulation of CD36 promotes the development of ccRCC. *Exp. Cell Res.* **421**, 113389 (2022).
22. S. Dehn *et al.*, HIF-2α in resting macrophages tempers mitochondrial reactive oxygen species to selectively repress MARCO–dependent phagocytosis. *J. Immunol.* **197**, 3639–3649 (2016).
23. Y. Luan *et al.*, Monocytic myeloid-derived suppressor cells accumulate in renal transplant patients and mediate CD4+Foxp3+ Treg expansion. *Am. J. Transpl.* **13**, 3123–3131 (2013).
24. T. Nakamura, T. Nakao, E. Ashihara, N. Yoshimura, Myeloid-derived suppressor cells recruit CD4+/Foxp3+ regulatory T cells in a murine cardiac allograft. *Transpl. Proc.* **48**, 1275–1278 (2016).
25. A. S. Chong, B cells as antigen-presenting cells in transplantation rejection and tolerance. *Cell. Immunol.* **349**, 104061 (2020).
26. W. Y. Kim *et al.*, Failure to prolyl hydroxylate hypoxia-inducible factor α phenocopies VHL inactivation in vivo. *EMBO J.* **25**, 4650–4662 (2006).
27. M. DeBerge *et al.*, Hypoxia-inducible factors individually facilitate inflammatory myeloid metabolism and inefficient cardiac repair. *J. Exp. Med.* **218**, e20200667 (2021).
28. R. Rojo *et al.*, Deletion of a Csf1r enhancer selectively impacts CSF1R expression and development of tissue macrophage populations. *Nat. Commun.* **10**, 3215 (2019).
29. N. Pescador *et al.*, Identification of a functional hypoxia-responsive element that regulates the expression of the egl nine homologue 3 (egln3/phd3) gene. *Biochem. J.* **390**, 189–197 (2005).
30. N. Chen *et al.*, Roxadustat for anemia in patients with kidney disease not receiving dialysis. *N Engl. J. Med.* **381**, 1001–1010 (2019).
31. S. Fishbane *et al.*, Roxadustat for treating anemia in patients with CKD not on dialysis: Results from a randomized phase 3 study. *J. Am. Soc. Nephrol.* **32**, 737–755 (2021).
32. J. A. Burke *et al.*, Subcutaneous nanotherapy repurposes the immunosuppressive mechanism of rapamycin to enhance allogeneic islet graft viability. *Nat. Nanotechnol.* **17**, 319–330 (2022).
33. S. Yi *et al.*, Surface engineered polymersomes for enhanced modulation of dendritic cells during cardiovascular immunotherapy. *Adv. Funct. Mater.* **29**, 1904399 (2019).
34. U. D. Balzo *et al.*, Nonclinical characterization of the hypoxia-inducible factor prolyl hydroxylase inhibitor roxadustat, a novel treatment of anemia of chronic kidney disease. *J. Pharmacol. Exp. Therapeutics* **374**, 342–353 (2020).
35. G. Hoppe *et al.*, Comparative systems pharmacology of HIF stabilization in the prevention of retinopathy of prematurity. *Proc. Natl. Acad. Sci. U.S.A.* **113**, E2516–E2525 (2016).
36. P. Björck, P. T. H. Coates, Z. Wang, F. J. Duncan, A. W. Thomson, Promotion of long-term heart allograft survival by combination of mobilized donor plasmacytoid dendritic cells and anti-CD154 monoclonal antibody. *J. Heart Lung Transpl.* **24**, 1118–1120 (2005).
37. T. Oda *et al.*, Hypoxia-inducible factor-1α expression in kidney transplant biopsy specimens after reperfusion is associated with early recovery of graft function after cadaveric kidney transplantation. *Transpl. Proc.* **49**, 68–72 (2017).
38. M. A. I. Keränen *et al.*, Cardiomyocyte-targeted HIF-1alpha gene therapy inhibits cardiomyocyte apoptosis and cardiac allograft vasculopathy in the rat. *J. Heart Lung Transpl.* **29**, 1058–1066 (2010).
39. R. J. Appelhoff *et al.*, Differential function of the prolyl hydroxylases PHD1, PHD2, and PHD3 in the regulation of hypoxia-inducible factor*. *J. Biol. Chem.* **279**, 38458–38465 (2004).
40. O. Zolk, T. F. Solbach, T. Eschenhagen, A. Weidemann, M. F. Fromm, Activation of negative regulators of the hypoxia-inducible factor (HIF) pathway in human end-stage heart failure. *Biochem. Biophys. Res. Commun.* **376**, 315–320 (2008).
41. F. Gramley *et al.*, Hypoxia and myocardial remodeling in human cardiac allografts: A time-course study. *J. Heart Lung Transpl.* **28**, 1119–1126 (2009).
42. X. Jiang *et al.*, Endothelial hypoxia-inducible factor-2α is required for the maintenance of airway microvasculature. *Circulation* **139**, 502–517 (2019).
43. M. A. I. Keränen *et al.*, Hypoxia-inducible factor controls immunoregulatory properties of myeloid cells in mouse cardiac allografts – an experimental study. *Transpl. Int.* **32**, 95–106 (2019).
44. E. Conde *et al.*, Hypoxia inducible factor 1-alpha (HIF-1 alpha) is induced during reperfusion after renal ischemia and is critical for proximal tubule cell survival. *PLoS One* **7**, e33258 (2012).
45. P. Koivunen, M. Hirsilä, V. Günzler, K. I. Kivirikko, J. Myllyharju, Catalytic properties of the asparaginyl hydroxylase (FIH) in the oxygen sensing pathway are distinct from those of its prolyl 4-hydroxylases. *J. Biol. Chem.* **279**, 9899–9904 (2004).
46. B. J. Kopecky *et al.*, Role of donor macrophages after heart and lung transplantation. *Am. J. Transpl.* **20**, 1225–1235 (2020).
47. M. Nahrendorf, M. J. Pittet, F. K. Swirski, Monocytes: Protagonists of infarct inflammation and repair after myocardial infarction. *Circulation* **121**, 2437–2445 (2010).
48. K. Furuichi *et al.*, CCR2 signaling contributes to ischemia-reperfusion injury in kidney. *J. Am. Soc. Nephrol.* **14**, 2503–2515 (2003).
49. T. Abe *et al.*, Graft-derived CCL2 increases graft injury during antibody-mediated rejection of cardiac allografts. *Am. J. Transpl.* **14**, 1753–1764 (2014).
50. M. Miura, T. El-Sawy, R. L. Fairchild, Neutrophils mediate parenchymal tissue necrosis and accelerate the rejection of complete major histocompatibility complex-disparate cardiac allografts in the absence of interferon-gamma. *Am. J. Pathol.* **162**, 509–519 (2003).
51. K. Morita *et al.*, Early chemokine cascades in murine cardiac grafts regulate T cell recruitment and progression of acute allograft rejection1. *J. Immunol.* **167**, 2979–2984 (2001).
52. D. G. Healy *et al.*, Neutrophil transendothelial migration potential predicts rejection severity in human cardiac transplantation. *Eur. J. Cardio-Thoracic Surgery* **29**, 760–766 (2006).
53. B. J. Kopecky *et al.*, Donor macrophages modulate rejection after heart transplantation. *Circulation* **146**, 623–638 (2022).
54. S. Watanabe, M. Alexander, A. V. Misharin, G. R. S. Budinger, The role of macrophages in the resolution of inflammation. *J. Clin. Invest.* **129**, 2619–2628 (2019).
55. K. J. Lavine *et al.*, The macrophage in cardiac homeostasis and disease. *J. Am. College Cardiol.* **72**, 2213–2230 (2018).
56. P. Chaturvedi, D. M. Gilkes, N. Takano, G. L. Semenza, Hypoxia-inducible factor-dependent signaling between triple-negative breast cancer cells and mesenchymal stem cells promotes macrophage recruitment. *Proc. Natl. Acad. Sci. U.S.A.* **111**, E2120–E2129 (2014).
57. A. S. M. R. Haque *et al.*, CD206+ tumor-associated macrophages promote proliferation and invasion in oral squamous cell carcinoma via EGF production. *Sci. Rep.* **9**, 14611 (2019).
58. S. Greenbaum *et al.*, A spatially resolved timeline of the human maternal–fetal interface. *Nature* **619**, 595–605 (2023).
59. J.-Y. Sun *et al.*, Placental immune tolerance and organ transplantation: Underlying interconnections and clinical implications. *Front. Immunol.* **12**, 705950 (2021).
60. J. C. Ochando, S. H. Chen, Myeloid-derived suppressor cells in transplantation and cancer. *Immunol. Res.* **54**, 275–285 (2012).
61. J. L. Bowser, J. W. Lee, X. Yuan, H. K. Eltzschig, The hypoxia-adenosine link during inflammation. *J. Appl. Physiol.* **123**, 1303–1320 (2017).
62. W. Ruan *et al.*, Targeting myocardial equilibrative nucleoside transporter ENT1 provides cardioprotection by enhancing myeloid Adora2b signaling. *JCI Insight* **8**, e166011 (2023).
63. K. Varani *et al.*, Changes of peripheral A2A adenosine receptors in chronic heart failure and cardiac transplantation. *FASEB J.* **17**, 280–282 (2003).
64. R. T. Smolenski *et al.*, Protection from reperfusion injury after cardiac transplantation by inhibition of adenosine metabolism and nucleotide precursor supply. *Circulation* **104**, I-246–I-252 (2001).
65. S. Hyun Lim *et al.*, Adenosine injection prior to cardioplegia enhances preservation of senescent hearts in rat heterotopic heart transplantation. *Eur. J. Cardio-Thoracic Surgery* **43**, 1202–1208 (2012).
66. H. Ehrentraut, J. A. Westrich, H. K. Eltzschig, E. T. Clambey, Adora2b adenosine receptor engagement enhances regulatory T cell abundance during endotoxin-induced pulmonary inflammation. *PLOS One* **7**, e32416 (2012).
67. M. Koeppen *et al.*, Hypoxia-inducible factor 2-alpha-dependent induction of amphiregulin dampens myocardial ischemia-reperfusion injury. *Nat. Commun.* **9**, 816 (2018).
68. N. Arpaia *et al.*, A distinct function of regulatory T cells in tissue protection. *Cell* **162**, 1078–1089 (2015).
69. D. Burzyn *et al.*, A special population of regulatory T cells potentiates muscle repair. *Cell* **155**, 1282–1295 (2013).
70. T.-S. Hsu *et al.*, HIF-2α is indispensable for regulatory T cell function. *Nat. Commun.* **11**, 5005 (2020).
71. J. W. Lee *et al.*, Transcription–independent induction of ERBB1 through hypoxia-inducible factor 2A provides cardioprotection during ischemia and reperfusion. *Anesthesiology* **132**, 763–780 (2020).
72. N. Chen *et al.*, Roxadustat treatment for anemia in patients undergoing long-term dialysis. *N Engl. J. Med.* **381**, 1011–1022 (2019).
73. W. M. Bernhardt *et al.*, Donor treatment with a PHD-inhibitor activating HIFs prevents graft injury and prolongs survival in an allogenic kidney transplant model. *Proc. Natl. Acad. Sci. U.S.A.* **106**, 21276–21281 (2009).
74. C. Heim *et al.*, Prolyl-hydroxylase inhibitor activating hypoxia-inducible transcription factors reduce levels of transplant arteriosclerosis in a murine aortic allograft model. *Interact. Cardiovasc. Thorac. Surg.* **22**, 561–570 (2016).
75. A. Toschi, E. Lee, N. Gadir, M. Ohh, D. A. Foster, Differential dependence of hypoxia-inducible factors 1 alpha and 2 alpha on mTORC1 and mTORC2 *. *J. Biol. Chem.* **283**, 34495–34499 (2008).
76. A. D. Wells *et al.*, Requirement for T-cell apoptosis in the induction of peripheral transplantation tolerance. *Nat. Med.* **5**, 1303–1307 (1999).
77. J. M. O *et al.*, Using mTOR inhibitor nanoimmunotherapy to induce cardiac allograft tolerance in non-human primates. *J. Heart Lung Transpl.* **41**, S148–S149 (2022).
78. T. Wu *et al.*, mTOR masters monocytic myeloid-derived suppressor cells in mice with allografts or tumors. *Sci. Rep.* **6**, 20250 (2016).
79. Y. Deng *et al.*, mTOR-mediated glycolysis contributes to the enhanced suppressive function of murine tumor-infiltrating monocytic myeloid-derived suppressor cells. *Cancer Immunol. Immunotherapy* **67**, 1355–1364 (2018).
80. X. Ding, H. Du, M. C. Yoder, C. Yan, Critical role of the mTOR pathway in development and function of myeloid-derived suppressor cells in Ial−/− mice. *Am. J. Pathol.* **184**, 397–408 (2014).
81. L. Xie *et al.*, Hypoxia-inducible factor/MAZ-dependent induction of caveolin-1 regulates colon permeability through suppression of occludin, leading to hypoxia-induced inflammation. *Mol. Cell. Biol.* **34**, 3013–3023 (2014).
82. T. Hasegawa, S. H. Visovatti, M. C. Hyman, T. Hayasaki, D. J. Pinsky, Heterotopic vascularized murine cardiac transplantation to study graft arteriopathy. *Nat. Protoc.* **2**, 471–480 (2007).
83. K. Glinton *et al.*, Bone marrow-derived AXL tyrosine kinase promotes mitogenic crosstalk and cardiac allograft vasculopathy. *J. Heart Lung Transplant.* **40**, 435–446 (2021).
84. M. L. Miller *et al.*, Spontaneous restoration of transplantation tolerance after acute rejection. *Nat. Commun.* **6**, 7566 (2015).
85. S. H. Khiew *et al.*, Transplantation tolerance modifies donor-specific B cell fate to suppress de novo alloreactive B cells. *J. Clin. Invest.* **130**, 3453–3466 (2020).
86. M. DeBerge *et al.*, Hypoxia Inducible Factor 2 promotes tolerogenic macrophage development during cardiac transplantation through transcriptional regulation of colony stimulating factor 1 receptor. NCBI Gene Expression Omnibus. https://www.ncbi.nlm.nih.gov/geo/query/acc.cgi?acc=GSE262851. Deposited 30 March 2024